This article is a *Plant Cell* Advance Online Publication. The date of its first appearance online is the official date of publication. The article has been edited and the authors have corrected proofs, but minor changes could be made before the final version is published. Posting this version online reduces the time to publication by several weeks.

Non-Cell-Autonomous Postmortem Lignification of Tracheary Elements in *Zinnia elegans*[W][OA]

Edouard Pesquet,[a,1] Bo Zhang,[a] András Gorzsás,[b,2] Tuula Puhakainen,[a,3] Henrik Serk,[a] Sacha Escamez,[a] Odile Barbier,[c] Lorenz Gerber,[b] Charleen Courtois-Moreau,[a,4] Edward Alatalo,[d] Lars Paulin,[d] Jaakko Kangasjärvi,[e] Björn Sundberg,[b] Deborah Goffner,[c] and Hannele Tuominen[a]

[a] Umeå Plant Science Centre, Department of Plant Physiology, Umeå University, 901 87 Umea, Sweden
[b] Umeå Plant Science Centre, Department of Forest Genetics and Plant Physiology, Swedish University of Agricultural Sciences, 901 83 Umea, Sweden
[c] Unité Mixte de Recherche 5546, Centre National de la Recherche Scientifique–Université Paul Sabatier, Surfaces Cellulaires et Signalisation Chez les Végétaux, 31326 Castanet-Tolosan, France
[d] DNA Sequencing and Genomics, Institute of Biotechnology, University of Helsinki, 00014 Helsinki, Finland
[e] Plant Biology, Department of Biological and Environmental Sciences, University of Helsinki, 00014 Helsinki, Finland

Postmortem lignification of xylem tracheary elements (TEs) has been debated for decades. Here, we provide evidence in *Zinnia elegans* TE cell cultures, using pharmacological inhibitors and in intact *Z. elegans* plants using Fourier transform infrared microspectroscopy, that TE lignification occurs postmortem (i.e., after TE programmed cell death). In situ RT-PCR verified expression of the lignin monomer biosynthetic cinnamoyl CoA reductase and cinnamyl alcohol dehydrogenase in not only the lignifying TEs but also in the unlignified non-TE cells of *Z. elegans* TE cell cultures and in living, parenchymatic xylem cells that surround TEs in stems. These cells were also shown to have the capacity to synthesize and transport lignin monomers and reactive oxygen species to the cell walls of dead TEs. Differential gene expression analysis in *Z. elegans* TE cell cultures and concomitant functional analysis in *Arabidopsis thaliana* resulted in identification of several genes that were expressed in the non-TE cells and that affected lignin chemistry on the basis of pyrolysis–gas chromatography/mass spectrometry analysis. These data suggest that living, parenchymatic xylem cells contribute to TE lignification in a non-cell-autonomous manner, thus enabling the postmortem lignification of TEs.

INTRODUCTION

Xylem tracheary elements (TEs) represent key anatomical features acquired by plants during evolution to survive and colonize the harsh conditions of terrestrial habitats, allowing for both water conduction throughout the plant body and mechanical support (Kenrick and Crane, 1997). Xylem vessels are formed by the assembly into files of TEs, which differentiate in a coordinated fashion to ensure continuous vascular connection from roots to leaves. TE differentiation includes deposition of secondary cell wall and programmed cell death (PCD), which results in the formation of a functional cell corpse devoid of cytoplasm. TE secondary cell walls are reinforced by lignin, a polyphenolic polymer, which confers both impermeability that is necessary for the efficient transport of water and physical strength against the surrounding tissues. Modification of lignin biosynthesis by genetic or pharmacological means results in weakened stems due to collapse of the xylem vessel secondary cell walls (Smart and Amrhein, 1985; Jones et al., 2001; Thévenin et al., 2011). Lignin results from the oxidative radical coupling of several different 4-hydroxyphenylpropene alcohol monomers, monolignols, which differ in the degree of methoxylation of the aromatic ring. The most common monomers are the non-methoxylated *para*-coumaryl alcohol, the monomethoxylated coniferyl alcohol, and the bimethoxylated sinapyl alcohol, giving H (hydroxyphenyl), G (guaicyl), and S (syringyl) units, respectively, in the lignin polymer (Boerjan et al., 2003; Ralph, 2010; Vanholme et al., 2012).

It was speculated early on that lignification of TEs in angiosperms occurs at least partially after apoptotic cell death or senescence of the xylem elements (for instance, see Stewart, 1966; Donaldson, 2001), but no efforts were taken to simultaneously track the dynamics of lignin deposition and TE viability. Radiolabeled phenylpropanoids have been applied to plant tissues to study the chronology of lignin precursor incorporation into the secondary walls of TEs. ^{3}H-labeled cinnamic acid was shown to be incorporated both in apparently living but also in dead xylem vessel elements of wheat (*Triticum aestivum*) coleoptiles (Pickett-Heaps, 1968), and even though somewhat contradictory results were obtained in another study in sycamore vessel elements (Wooding, 1968), it seems that addition of lignin precursors to

[1] Address correspondence to edouard.pesquet@plantphys.umu.se.
[2] Current address: Department of Chemistry, Umeå University, 901 87 Umea, Sweden.
[3] Current address: Department of Agricultural Sciences, University of Helsinki, 00014 Helsinki, Finland.
[4] Current address: Roche Diagnostics Deutschland, Sandhofer Strasse 116, 68305 Mannheim, Germany.
The author responsible for distribution of materials integral to the findings presented in this article in accordance with the policy described in the Instructions for Authors (www.plantcell.org) is: Edouard Pesquet (edouard.pesquet@plantphys.umu.se).
[W] Online version contains Web-only data.
[OA] Open Access articles can be viewed online without a subscription.
www.plantcell.org/cgi/doi/10.1105/tpc.113.110593

already lignified cells can further enhance accumulation of lignin even after death of the vessel elements. Similar conclusions were drawn from studies performed in *Zinnia elegans* TE cell cultures in which reduction in TE lignification by pharmacological inhibitors could be compensated for by the addition of lignin monomers to TEs undergoing lignification (Sato et al., 1993; Hosokawa et al., 2001; Tokunaga et al., 2005). However, none of these studies provided experimental evidence on how lignification relates to cell death of TEs. It was therefore very interesting that bulk deposition of lignin was recently shown to occur postmortem (i.e., after TE cell death) by live-cell imaging of differentiating *Arabidopsis thaliana* TEs, although the interdependency, if any, of TE PCD and lignification was not experimentally tested (Pesquet et al., 2010, Pesquet and Lloyd, 2011). Our specific research question is therefore whether lignification in TEs occurs independently of cell death and how these processes affect each other to enable the formation of a functional, lignified TE.

Lignin monomers are considered to be synthesized in a cell-autonomous manner in the lignifying TEs and exported to the cell wall by ABC transporters (Miao and Liu, 2010; Alejandro et al., 2012) and vesicles (Liu, 2012). Postmortem lignification implies that TE lignification occurs either due to the release of

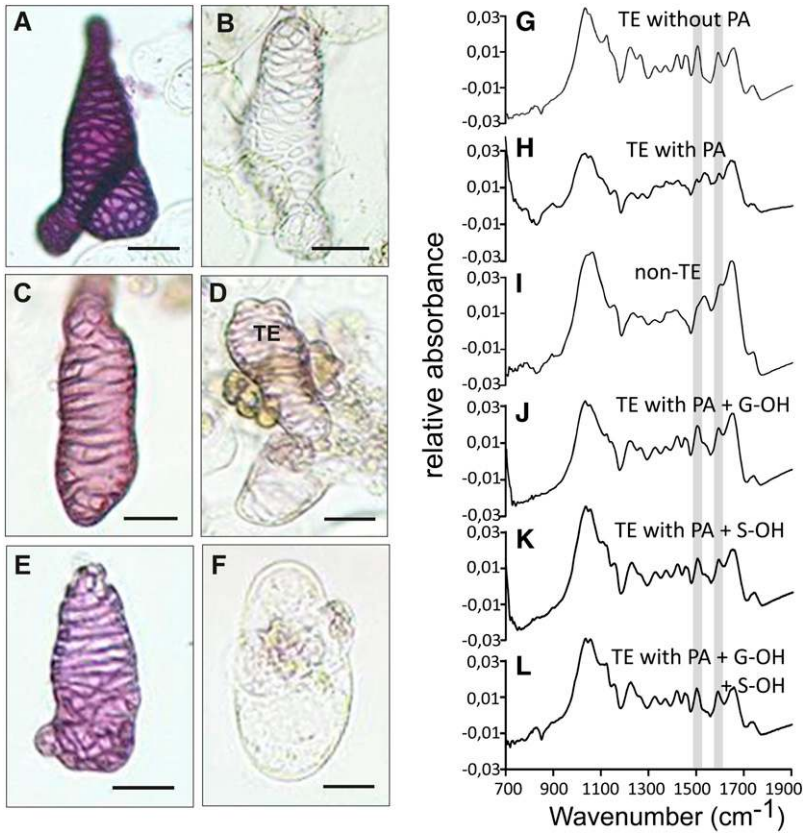

Figure 1. Postmortem Lignification of *Z. elegans* TEs.

(A) to **(F)** Phloroglucinol-HCl staining of 168-h-old dead TEs. Bars = 10 μm.
(A) A typical control TE not treated with PA.
(B) A typical TE treated with 50 μM PA.
(C) A typical TE treated with 50 μM PA and supplemented with 60 μM coniferyl alcohol.
(D) A typical TE treated with 50 μM PA and supplemented with 60 μM sinapyl alcohol.
(E) A typical TE treated with 50 μM PA and supplemented with both 60 μM coniferyl and 60 μM sinapyl alcohol.
(F) A typical non-TE cell treated with 50 μM PA and supplemented with 60 μM coniferyl alcohol.
(G) to **(L)** Average FT-IR spectra of single 168-h-old dead TEs after different treatments. n = 8 to 12 independent cells taken from three independent biological replicates. Lignin-specific bands at 1510 and 1595 cm^{-1} are indicated with gray bars.
(G) Control TEs not treated with PA.
(H) TEs treated with 50 μM PA.
(I) Untreated non-TE cells.
(J) TEs treated with 50 μM PA and supplemented with 60 μM coniferyl alcohol (G-OH).
(K) TEs treated with 50 μM PA and supplemented with 60 μM sinapyl alcohol (S-OH).
(L) TEs treated with 50 μM PA and supplemented with both 60 μM coniferyl alcohol (G-OH) and 60 μM sinapyl alcohol (S-OH).

monolignols from dying TEs and/or in a non-cell-autonomous manner in which other cells are required to achieve full lignification of TEs after their death. Several observations support non-cell-autonomous TE lignification. For instance, a number of genes that have been associated with lignin monomer biosynthesis have been shown to be expressed not only in living TEs but also in the cambium and the ray parenchyma cells of xylem (Hu et al., 1998; Chen et al., 2000; Lacombe et al., 2000; Lauvergeat et al., 2002; Baghdady et al., 2006). Also, it has been shown that lignification continues in *Z. elegans* in vitro TE culture long after the death of the TEs (Hosokawa et al., 2001), supporting the function of the remaining living, parenchymatic cells in TE cultures in postmortem lignification of dead TEs. For these reasons, a reexamination of the level of cell autonomy/cooperativity during TE lignification is necessary.

In this study, we have taken pharmacological and genetic approaches to experimentally define the spatio-temporal relationship of TE PCD and lignification and to examine the extent of cell autonomy during TE lignification in cell cultures and intact plants of *Z. elegans* and in *Arabidopsis* plants. The use of xylogenic cell cultures enabled pharmacological modifications and monitoring of TE PCD and/or lignification without interference with other developmental processes or compensatory mechanisms that often take place when TE maturation is modified in whole plants. Experiments in TE cell cultures and intact plants of *Z. elegans* provided evidence for non-cell-autonomous postmortem lignification. Differential gene expression analysis in TE cell cultures and concomitant functional analysis in planta supported function of the neighboring parenchymatic cells in TE lignification and allowed identification of genes that might be involved in this process.

RESULTS

Experimental Evidence for Postmortem TE Lignification

The relationship between TE lignification and cell death was analyzed experimentally in differentiating *Z. elegans* TE cell cultures that were treated at the beginning of the cell culture period with a pharmacological inhibitor of lignin monomer biosynthesis, piperonylic acid (PA). PA is an inactivator of cinnamate-4-hydroxylase that catalyzes the 4-hydroxylation of the aromatic ring of monolignol precursors (Schalk et al., 1998; Schoch et al., 2002). Cell wall lignification of 120-h-old TEs was first estimated using lignin-specific phloroglucinol-HCl staining. The control cultures resulted in dead and lignified TEs (Figure 1A), whereas the 25 to 50 μM PA-treated cultures resulted in unlignified dead TEs devoid of protoplasm (Figure 1B). Chemical fingerprints of TE cell walls were obtained by Fourier transform infrared (FT-IR) microspectroscopy (Gorzsás et al., 2011). The average FT-IR spectra of single TE cells revealed characteristic lignin bands at 1510 and 1595 cm^{-1} (Faix, 1991) in the control TEs without added PA (Figure 1G). These specific bands were largely absent in the TEs treated with PA (Figure 1H) and in non-TE cells (Figure 1I), appearing only as small shoulders on large neighboring bands. Interestingly, when supplying the PA-treated TEs with pure coniferyl alcohol (G-type) lignin monomers, the TEs were capable of lignifying postmortem within the next 24 to 48 h (Figures 1C and 1J). Similarly, adding sinapyl alcohol (S-type) lignin monomers alone or at a 1-to-1 ratio with G-type monomers enabled complete lignification postmortem of the dead PA-treated TEs (Figures 1D, 1E, 1K, and 1L), while the PA-treated non-TE cells remained unlignified (Figure 1F). Multivariate analysis and hierarchical clustering of FT-IR profiles showed that

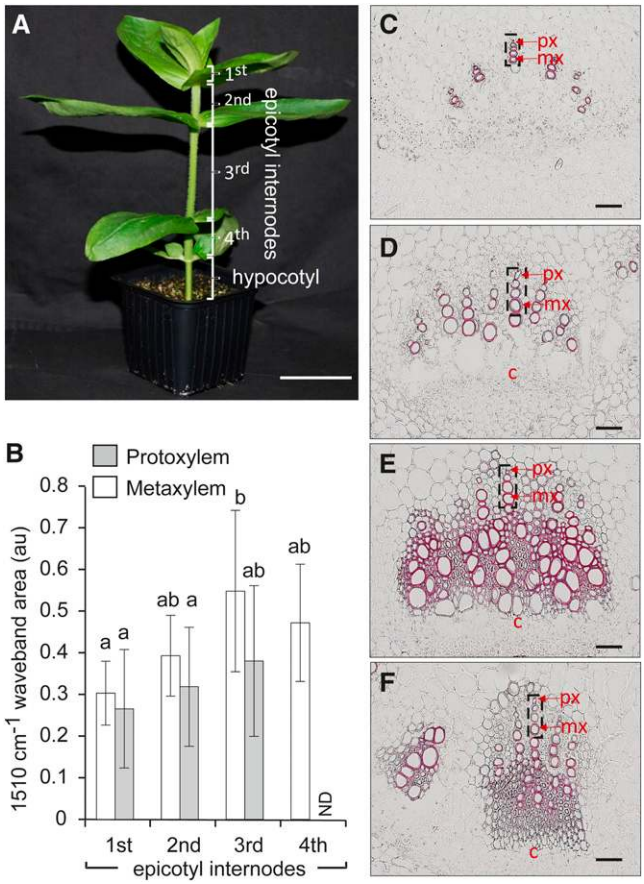

Figure 2. Progression of Xylem TE Lignification in Whole *Z. elegans* Plants.

(A) Transverse sections were taken from 5-week-old *Zinnia elegans* plants from the 1st to the 4th epicotyl internode, as indicated, for FT-IR microspectroscopy analysis. Bar = 3 cm.

(B) Average peak area of the 1510 cm^{-1} band (aromatic –C=C– vibration associated to G-type lignin in au, arbitrary units), calculated using infrared spectra from 17 to 24 independent protoxylem and metaxylem vessels in the different internodes of four biological replicates. The protoxylem vessels of the 4th internode were crushed and could not be detected reliably (ND, nondetectable). Vertical bars indicate ±SD. Samples are significantly different from each other when labeled with distinct letters on the basis of a post-ANOVA Tukey test.

(C) to **(E)** Phloroglucinol-HCl staining of 20-μm-thick cross sections of the various epicotyl internode segments from the 1st **(C)**, 2nd **(D)**, 3rd **(E)**, and 4th internode **(F)**. In red, c indicates the cambium, mx the metaxylem vessels, and px the protoxylem vessels, and the boxed area marks the primary xylem positions used for the FT-IR microspectroscopy analysis. Bars = 400 μm.

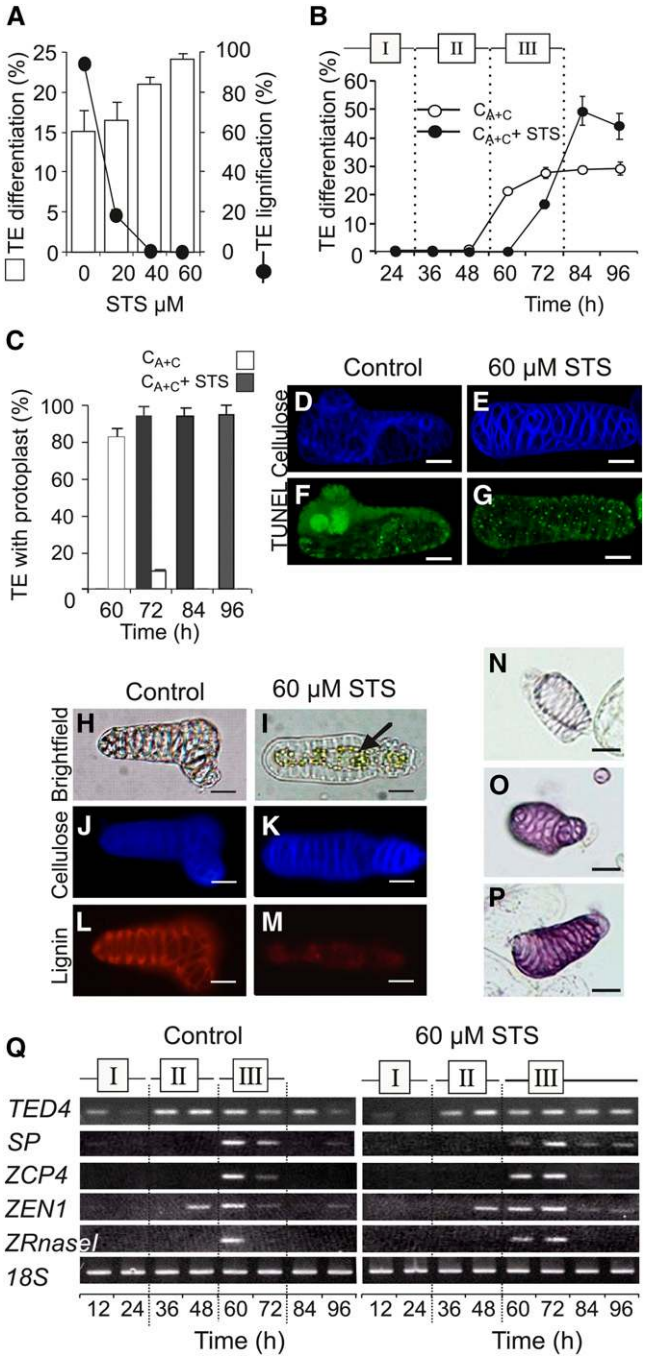

Figure 3. Arrest of *Z. elegans* TE Lignification and Cell Death by STS.

(A) Overall effect of STS treatment on TE differentiation efficiency (expressed as a percentage of TEs out of all cells) and on TE lignification (expressed as a percentage of lignified TEs out of all TEs) after 120 h of culture. Vertical bars indicate ±SD.

(B) Effect of STS on TE differentiation efficiency along the time course (expressed as a percentage of TEs out of all cells). The three successive phases of TE differentiation, loss of mesophyll status (I), acquirement of xylogenic potency (II), and TE maturation (III) are indicated along the time course. Vertical bars indicate ±SD.

supplying PA-treated TEs with a combination of both G- and S-type monomers resulted in cell wall chemistry that was most similar to the ones in the control in vitro TEs without PA and in TEs obtained from macerated *Z. elegans* stems (see Supplemental Figures 1A to 1C online). This is consistent with the fact that the *Z. elegans* TEs are composed of mostly G-type but also to a lower extent of S-type lignin residues, as shown by thioacidolysis and histochemical Maüle analyses (see Supplemental Figures 1D and 1E online). Altogether, these results provide experimental evidence for postmortem lignification of TEs.

Postmortem lignification requires production and export of monolignols into the apoplastic space. To examine the presence of lignin monomers in the apoplastic space under normal culture conditions, filtered culture medium from 120-h-old TE cell cultures was provided to replace the medium of the PA-treated TEs. Under these conditions, lignification of the PA-treated TEs was achieved only when adding the extracellular medium from cell cultures that were initially induced to form TEs by the addition of both auxin and cytokinin but not from uninduced control cell cultures supplied only with auxin, cytokinin, or no hormone (see Supplemental Figures 1F to 1K online). This confirms that the normal TE cell cultures that are induced to become TEs produce and export monolignols in the apoplastic space for TEs to lignify. Altogether, these results demonstrate that TEs can fully lignify after their death if supplied with appropriate monomers. Moreover, the fact that secondary cell walls can lignify postmortem implies that the

(C) Overall effect of STS on the lifetime of the TEs (expressed as a percentage of TEs with vestigial protoplast out of all TEs). Vertical bars indicate ±SD.

(D) to **(G)** TUNEL staining of control TEs (**[D]** and **[F]**) and STS-treated TEs (**[E]** and **[G]**) during TE maturation in phase III. TEs were visualized by confocal imaging of calcofluor-stained cellulosic secondary walls (**[D]** and **[E]**) and FITC fluorescence of the TUNEL-labeled DNA (**[F]** and **[G]**). TUNEL-labeled nuclei are visible in two maturing control TEs **(F)**. Bars = 10 µm.

(H) to **(M)** Cell cytology in control TEs (**[H]**, **[J]**, and **[L]**) and STS-treated TEs (**[I]**, **[K]**, and **[M]**) after 120 h of culture. TEs were visualized by bright-field imaging (**[H]** and **[I]**), by calcofluor staining of the cellulosic cell walls (**[J]** and **[K]**), and by lignin autofluorescence (**[L]** and **[M]**). The arrow indicates the vestigial protoplast in the STS-treated TE. Bars = 8 µm.

(N) to **(P)** Effect of extracellular medium from STS-treated TE cell cultures on TE differentiation of PA-treated TEs. Bars = 10 µm.

(N) A typical 120-h-old TE treated with 50 µM PA.

(O) A typical 120-h-old TE treated with 50 µM PA and supplemented with 0.2 µM filtered extracellular medium from a normal 120-h-old TE cell culture.

(P) A typical 120-h-old TE treated with 50 µM PA and supplemented with 0.2 µM filtered extracellular medium from STS-treated 120-h-old TE cell culture.

(Q) RT-PCR expression analysis of *TRACHEARY ELEMENT DIFFERENTIATION4* (*TED4*), *Z. elegans SERINE PROTEASE* (*SP*), *ZCP4*, *ZEN1*, ZRnase1, and control *18S* rRNA along the TE differentiation time course in control and STS-treated cells. Expression of the phase II–specific *TED4* and of the phase III–specific *SP* (Fukuda, 1997; Pesquet and Tuominen, 2011) were analyzed to define the different phases of TE differentiation.

lignin-oxidizing enzymes are present and remain active in TE secondary walls even after the cell death.

Postmortem Lignification of TEs in Planta

To analyze whether TE lignification continues postmortem in planta, the amount of cell wall lignin was analyzed in protoxylem and metaxylem vessels of different ages by FT-IR microspectroscopy (Gorzsás et al., 2011). 16-μm-thick transversal cryosections were taken in the four first epicotyl internodes of 5-week-old *Z. elegans* plants (Figure 2A), and three to four consecutive proto- and metaxylem vessels were analyzed in the primary xylem of the vascular bundle (Figures 2C to 2F). Primary xylem vessels are easily distinguishable, exhibit secondary cell wall patterns similar to TEs in vitro, and are completely isolated from neighboring lignified cells (Pesquet et al., 2003, 2006). These cells also mature very rapidly after their formation, as revealed by the phloroglucinol-HCl staining of transverse sections from the different epicotyl internodes (Figures 2C to 2F). In older stem internodes, protoxylem vessels are often crushed by the surrounding tissue and are therefore difficult to distinguish (Figure 2F).

No significant differences were found when comparing the four different plants used for the analyses (see Supplemental Figure 2A online). However, clear separation could be observed when comparing the four different internodes that represent vessel elements of different ages (see Supplemental Figure 2B online). To quantify the content of lignin, the intensity of the G-type lignin-specific 1510-cm^{-1} band was recorded in the vessel elements. Within each internode, protoxylem vessels did not exhibit significantly reduced intensity of the 1510-cm^{-1} band compared with metaxylem vessels even though there was a tendency toward higher lignin content in the metaxylem than in the protoxylem. However, clear differences were present between the internodes. While the primary xylem of the oldest, fourth internode was not any more easily detectable, it was clear that the intensity of the 1510-cm^{-1} band increased significantly from the youngest, first internode to the third internode especially in the metaxylem vessels (Figure 2B). The increasing trend of proto- and metaxylem vessel lignification along with the aging of the cells supports TE postmortem lignification in planta.

Inhibition of TE PCD and Lignification by Silver Thiosulfate

To further understand the temporal relationship between lignification and TE cell death, an experimental condition was sought that would block both TE lignification and PCD. The addition of 60 μM silver thiosulfate (STS), a known ethylene signaling inhibitor, to TE cultures resulted in complete inhibition of TE lignification (Figure 3A). STS also provoked a 12-h delay in the appearance of TEs (Figure 3B) and a slightly (10 to 15%) higher differentiation efficiency. Importantly, STS treatment also blocked TE PCD. Almost 100% of the STS-treated TEs retained their plasmolyzed protoplasts even 96 h after the TE induction, while 100% of the TEs in the control cultures without STS had already completely lost their protoplasts (Figure 3C). Analysis of nuclear DNA degradation patterns by terminal deoxynucleotidyl transferase dUTP nick end labeling (TUNEL) confirmed defective progression of TE cell death in response to STS (Figures 3D to 3G). Confocal microscopy imaging revealed that the STS treatment arrested TE maturation at a stage that was defined by normal deposition of the cellulosic secondary cell walls (Figures 3H to 3K) but without the overlying lignin deposition (Figures 3L and 3M). UV confocal spectroscopy confirmed that no lignin associated fluorescence could be detected in STS-treated cells (see Supplemental Figures 3A to 3I online). STS-treated TEs exhibited normal, transversely orientated cellulosic secondary cell walls but retained plasmolyzed vestigial protoplasts with individually separated organelles (Figure 3I). Although TE PCD progression was blocked by STS, expression of TE PCD marker genes *Z. elegans CYSTEINE PROTEASE4* (*ZCP4*), *Z. elegans ENDONUCLEASE1* (*ZEN1*), and *Z. elegans RIBONUCLEASE1* (*ZRnase1*) (Demura et al., 2002) was not suppressed but was instead extended (Figure 3Q).

It was not clear whether STS primarily affects TE cell death, lignification, or both. However, providing extracellular medium

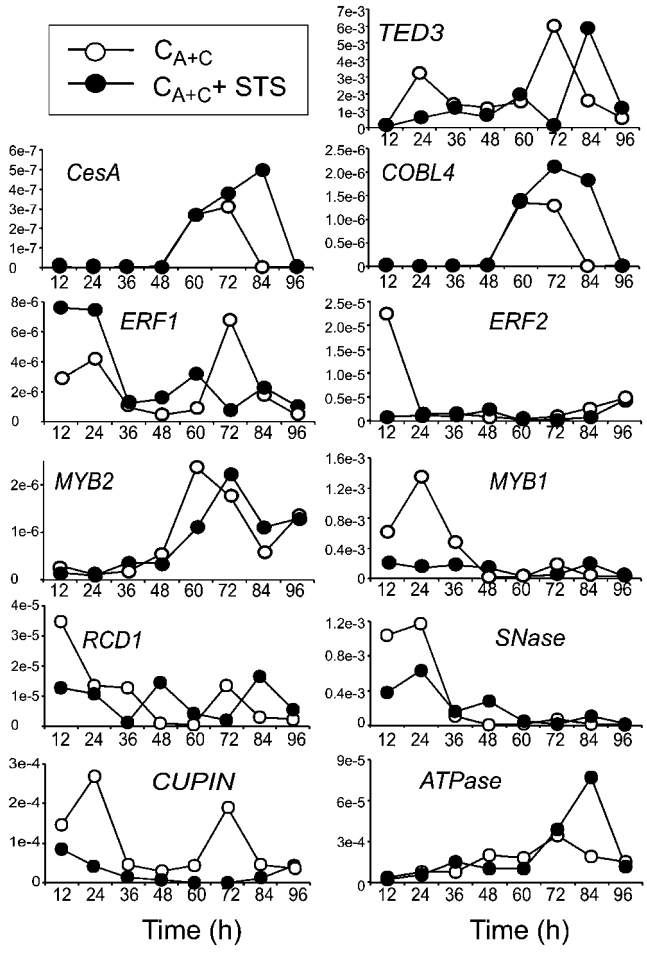

Figure 4. Identification of Transcriptional Changes Related to Postmortem TE Lignification in *Z. elegans* Cell Cultures.

Quantitative RT-PCR expression profiles of selected genes along the TE differentiation time course in control and 60 μM STS–treated *Z. elegans* TE cell cultures. For detailed description of the genes, see Supplemental Data Set 3 online. Values represent ratio of gene expression to the *18S* rRNA control.

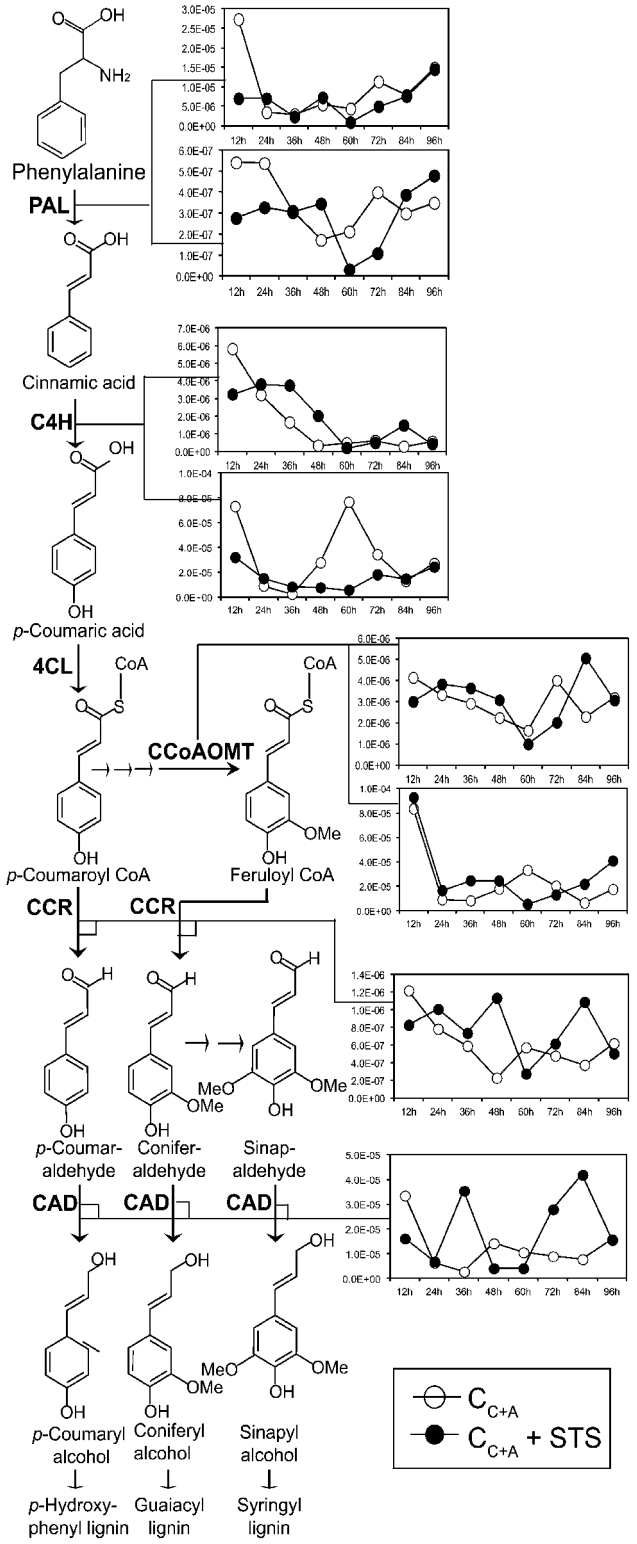

Figure 5. Expression of the Lignin Monomer Biosynthetic Genes in Response to STS Treatment in *Z. elegans* TE Cultures.

Quantitative RT-PCR expression profiles are shown for lignin biosynthetic genes along the TE differentiation time course in control and 60 μM STS–treated cells. For detailed description of the genes, see Supplemental Data Set 3 online. Values represent ratio of gene expression relative to the *18S* rRNA control.

from 120-h-old STS-treated TE cultures to PA-treated dead TEs enabled complete postmortem lignification (Figures 3N to 3P), demonstrating that monolignol production and polymerization were not inhibited by STS. Moreover, the addition of coniferyl alcohol to STS-treated TEs did not allow TEs to lignify. Altogether, these results suggest that STS primarily arrests TE PCD and that TE PCD is required to trigger polymerization of lignin monomers in the secondary cell walls.

Screening for Factors Involved in Postmortem TE Lignification

Simultaneous blocking of TE PCD and lignification by STS provided a condition in which to study molecular mechanisms underlying postmortem TE lignification. Two opposing suppression subtractive hybridization (SSH) libraries were therefore constructed from STS and control TE cell cultures prior to PCD to identify genes that were differentially expressed in response to STS treatment. A total of 2625 single pass sequences, clustered into 651 unique clusters, were generated from the two SSH libraries that were pooled together. The average sequence size was 315 ± 131 bp, ranging from 94 to 699 bp. A comprehensive gene list describing all aspects of the bioinformatic analysis is provided in Supplemental Data Set 1 online. Quantitative RT-PCR analysis revealed that many genes, exemplified here by the TE phase II marker *TED3* and the MYB transcription factor *MYB2*, showed a 12-h delay of their maximum expression level along the TE differentiation time course in response to STS treatment (Figure 4) that could be related to the STS-induced delay in TE differentiation. Expression of the cellulosic secondary cell wall–related cellulose synthase (*CesA*) and a COBRA-like4 protein was prolonged in response to STS in accordance with the prolonged TE lifespan in phase III (Figure 4). Expression of a few of the SSH library genes, such as the homologs of ethylene response factors (*ERF1* and *ERF2*), a cupin motif–containing protein (*CUPIN*), a MYB transcription factor (*MYB1*), and a mitochondrial F1 ATPase (*ATPase*), was either significantly suppressed or increased in STS-treated cultures (Figure 4). The SSH library also contained several other genes, such as the tudor domain–containing protein (*SNase*) and *RADICAL-INDUCED CELL DEATH1* (*RCD1*) (Figure 4) that were homologous to *Arabidopsis* proteins that have been implicated in various types of PCD processes (Overmyer et al., 2000; Sundström et al., 2009).

Expression of the Lignin Monomer Biosynthetic Genes in Non-TE Cells

The SSH libraries contained eight genes with a putative function in lignin monomer biosynthesis (see Supplemental Data Set 1 online). In the control culture, expression of most of these genes was slightly upregulated during TE maturation and continued

beyond the moment of TE PCD (beyond 72 h), while STS induced varying patterns of expression (Figure 5). For instance, the expression of a cinnamate-4-hydroxylase was significantly reduced during TE maturation in the presence of STS, while the downstream enzymes cinnamoyl CoA reductase (*CCR*) (exhibiting 80% protein sequence identity with *Arabidopsis* CCR1 [At1g15950]) and cinnamyl alcohol dehydrogenase (*CAD*) (exhibiting 65 to 68% protein sequence identity with *Arabidopsis* CAD4/C [At3g19450] and 5/D [At4g34230]) were upregulated in response to STS (Figure 5).

The expression of the lignin monomer biosynthesis genes beyond the moment of TE PCD raises a question about the localization of expression of these genes within *Z. elegans* cell cultures that are composed of both dying TEs and living non-TE cells (Fukuda and Komamine, 1980; Pesquet et al., 2005). To address this issue, the expression of *CCR* and *CAD* was localized by multiplex in situ RT-PCR both in *Z. elegans* cell cultures and in cross sections of *Z. elegans* stems. Localization of *CCR* and *CAD* expression in combination with *18S* rRNA control in *Z. elegans* cell cultures showed that *CCR* and *CAD* are expressed in both TEs and non-TE cells (Figures 6F, 6G, 6K, and 6L). The presence of two different cell types was confirmed by the localization of expression of a TE-specific marker *ZEN1* (Pesquet et al., 2004) that was clearly present only in differentiating TEs (Figure 6O), in comparison with *CCR*, which was expressed in both TEs and non-TE cells (Figure 6J). Similarly in *Z. elegans* stems, *CAD* and *CCR* were expressed in the non-TE cells surrounding xylem vessels of vascular bundles (i.e., xylem parenchyma) as well as in the cambium (see Supplemental Figure 4 online). Therefore, our results support earlier hypotheses (Hosokawa et al., 2001) that both TEs and non-TE cells in *Z. elegans* cell cultures and in stems express the genes to synthesize lignin monomers even though only the TEs lignify.

Production of Lignin Monomers in Non-TEs

The next question was whether the non-TE cells can also produce and secrete the phenolic compounds required for TE postmortem lignification. Cell cultures were grown in the presence of PA for 144 h, when all TEs were dead but nonlignified (Figure 1), to investigate the sole function of the remaining living non-TEs. At 144 h, the PA-treated TE cell cultures were washed three times with fresh medium and placed without any PA to remove the pharmacological inhibition. The washed cells were further incubated with or without PA for 24, 48, 72, and 96 h before visualizing TE secondary cell wall lignification state by phloroglucinol-HCl staining. In control cultures, 82% of the TEs were lignified (on the basis of intense staining by phloroglucinol-HCl), whereas PA-treated TEs remained completely unlignified (Figure 7A). Cell cultures that were first washed and then

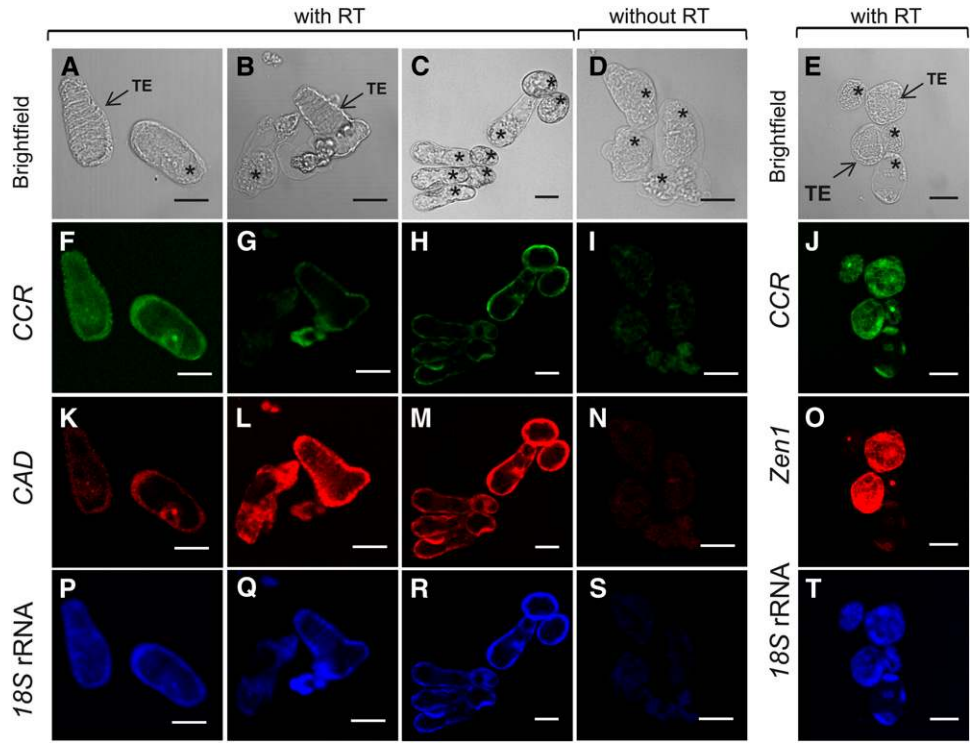

Figure 6. Multiplex in Situ RT-PCR of Lignin Monomer Biosynthetic Genes in *Z. elegans* TE Cell Cultures.

Expression of *CCR* (**[F]** to **[J]**), *CAD* (**[K]** to **[N]**), *ZEN1* **(O)**, and *18S* rRNA control (**[P]** to **[T]**) is shown in confocal images of 60-h-old TE cultures. For detailed description of the genes, see Supplemental Data Set 3 online. The cells are simultaneously visualized for bright-field transmission (**[A]** to **[E]**), FITC-labeled PCR amplicon (**[F]** to **[J]**), TMRA-labeled PCR amplicon (**[K]** to **[O]**), and Cy5 labeled PCR amplicon (**[P]** to **[T]**). Arrows indicate TEs that are defined either by cell morphology (**[A]** and **[B]**) or by *ZEN1*-specific expression **(O)**. Asterisks indicate non-TE cells. Bars = 8 μm.

supplemented with PA and 60 μM coniferyl alcohol comprised an average of 40% lignifed TEs after 24 h and remained approximately unchanged thereafter (Figure 7A). Cell cultures that were grown without PA after the wash exhibited a gradual increase in the degree of TE lignification from 24 to 96 h (Figure 7A), demonstrating that the non-TE cells can indeed produce and export monolignols for TE postmortem lignification.

Production of Reactive Oxygen Species in Non-TEs

Reactive oxygen species (ROS) have been shown to be required for full TE lignification (Karlsson et al., 2005; Ros Barceló, 2005). To define whether the ROS are produced by non-TEs, experiments were again conducted with the 144-h-old, PA-treated TE cell cultures that consisted of dead and non-lignified TEs and living non-TEs. At 144 h, cell cultures were washed three times with fresh medium and further incubated in fresh medium supplemented with PA and coniferyl alcohol as well as with or without pharmacological compounds affecting ROS production, such as the general cell permeable antioxidant and ROS scavenger *N*-acetylcysteine (NAC), the nonpermeable hydrogen peroxide hydrolyzing enzyme catalase (Cat), and NADPH oxidase inhibitor diphenylene iodonium (DPI). TEs that were incubated with only PA and coniferyl alcohol lignified postmortem (Figure 7B). NAC (1 mM) reduced significantly the number of postmortem lignified TEs (Figure 7B), most probably due to general inhibition of the oxidative polymerization of lignin. To specifically target ROS, treatments were performed with 15 μM DPI, which resulted in a significant reduction of postmortem lignified TEs, whereas 1 mg/mL Cat treatment reduced TE postmortem lignification, but to a lesser extent (Figure 7B). Our results are similar to those published by Karlsson et al. (2005), who treated *Z. elegans* TEs with similar compounds at 72 h while TEs were actively dying. Our results, together with the earlier findings, therefore indicate that non-TE cells indeed produce ROS which can affect TE postmortem lignification.

Identification of Non-TE Expressed Genes

To identify non-TE expressed genes that could operate in postmortem TE lignification, an in silico expression analysis of the SSH library genes was performed using publicly available *Z. elegans* as well as *Arabidopsis* in vitro TE expression data (Demura et al., 2002; Kubo et al., 2005). In these databases, 103 *Z. elegans* genes and 322 *Arabidopsis* genes homologous to the SSH sequences were identified (see Supplemental Figure 5 online). A gene was defined as being expressed in the non-TEs if it (1) was expressed in the cell culture time course beyond the TE PCD, which was between 72 and 84 h in *Z. elegans* (Demura et al., 2002) and between 8 and 10 d in *Arabidopsis* (Kubo et al., 2005); and (2) showed an expression level after TE PCD that was over 75% of the maximal expression during the TE lifetime. Out of all the homologous genes, 57.3% of the *Z. elegans* ESTs and 50% of the *Arabidopsis* genes fulfilled these criteria and were therefore considered non-TE expressed (see Supplemental Figure 5 online). Expression in non-TEs was verified for *Arabidopsis C4H*, *RCD1*, and *MYB13* with a β-glucuronidase (GUS) reporter analysis, which confirmed that all three genes were expressed in xylem parenchyma cells in immediate contact with xylem vessels in both vascular bundles of the stem and secondary xylem of the hypocotyl (Figure 8).

Reverse Genetic Analysis of Non-TE Expressed Genes

Functional characterization of a selected set of SSH library–derived *Z. elegans* genes was performed in *Arabidopsis* to

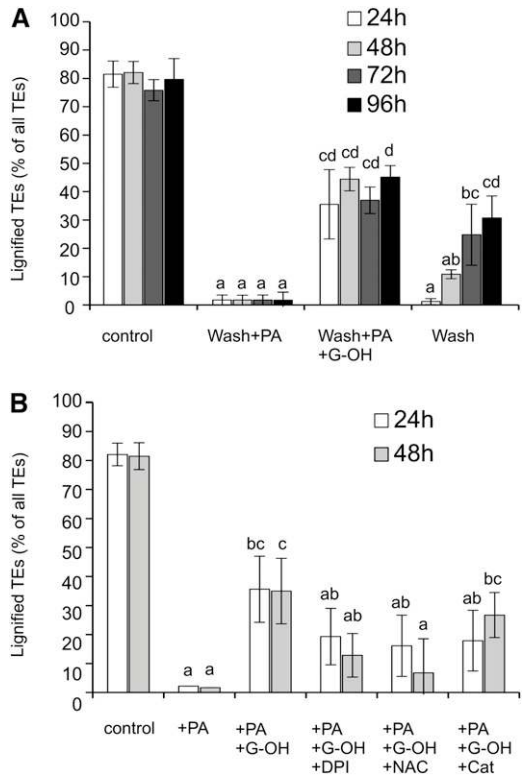

Figure 7. Cooperative TE Postmortem Lignification through Lignin Monomer and ROS Production by Non-TEs.

(A) The effect of non-TEs on postmortem TE lignification. *Z. elegans* TE cultures were initially treated with 50 μM PA and washed at 144 h and transferred to either fresh medium (Wash), 50 μM PA (Wash+PA), or 50 μM PA and 60 μM coniferyl alcohol (Wash+PA+G-OH). Control represents cultures that were not initially treated with PA. Lignification was estimated as the average percentage of phloroglucinol-positive TEs 1 to 4 d after the wash ± SD. Measurements were done in three independent biological replicates in which 50 to 60 TEs were measured in each. Samples are significantly different from each other when labeled with distinct letters on the basis of a post-ANOVA Tukey test.

(B) The effect of non-TE-produced ROS on TE postmortem lignification. *Z. elegans* TE cultures were initially treated with 50 μM PA, washed at 144 h, and treated further with either 50 μM PA (+PA) or 50 μM PA and 60 μM coniferyl alcohol (+PA+G-OH) supplemented or not with either 1 mM NAC, 15 μM DPI, or 1 mg/mL of Cat. Control represents cultures that were not initially treated with PA. Lignification was estimated as the average percentage of phloroglucinol-positive TEs ± SD 2 d after the wash. Measurements were done in three independent biological replicate in which 50 to 60 TEs were measured in each. Samples are significantly different from each other when labeled with distinct letters on the basis of a post-ANOVA Tukey test.

decipher whether these genes affected xylem lignification. The most similar *Arabidopsis* gene was identified for 49 randomly selected *Z. elegans* genes that were not previously associated with lignification (see Supplemental Data Set 1 online). These genes were further subdivided into two categories: 20 of them were considered non-TE expressed, whereas the rest were more specific to TEs (see Supplemental Data Set 2 online). Homozygous T-DNA mutants in each of these *Arabidopsis* genes were analyzed for cell wall chemistry in mature hypocotyls using pyrolysis–gas chromatography/mass spectrometry (Py-GC/MS). The analysis yielded chemical fingerprints consisting of 127 pyrolytic degradation products from the cell wall carbohydrates (cellulose and hemicellulose) and lignin (Gerber et al., 2012). Two mutants in lignin monomer biosynthesis, *c4h-3/ref3.3* (Ruegger and Chapple, 2001) and *ccr1-3* (Mir Derikvand et al., 2008), were included as controls (both also affected by STS and expressed in non-TE cells). The complete list of the genes and the mutants and the statistical analysis of the Py-GC/MS results can be found in Supplemental Data Set 2 online. In this analysis, only 20 among the 49 mutants separated well (Q2 > 0.5) from the wild type using multivariate analysis (see Supplemental Data Set 2 online). Interestingly, 12 of these 20 genes were considered to be non-TE expressed (see Supplemental Data Set 2 online). These included two mutant alleles of *RCD1* (At1g32230), several unknown genes (At5g20130, At2g25660, and At5g05190), the *MYB13* transcription factor (At1g06180), and a putative cobalamin biosynthetic protein (*CBP*; At1g26520). Among these mutants, quantitative analysis revealed statistically significant differences in three mutants for the relative amount of G-type lignin, in three mutants for the relative amount of H-type lignin, and in four mutants for the total lignin content (Figure 9A). Most significant changes were observed in *rcd1* and *myb13* mutants. None of the mutants differed significantly from the wild type in terms of growth, xylem anatomy, or lignin distribution (Figures 9B and 9C; see Supplemental Figure 6 online) except for *rcd1* and to a lesser extent *cbp*, which were smaller in size (Figure 9B; see Supplemental Figures 6N and 6R online). Altogether, these results suggest that non-TE expressed genes can modulate lignification of xylem in whole plants, although further studies are needed to address precisely the role of these genes in xylem lignification.

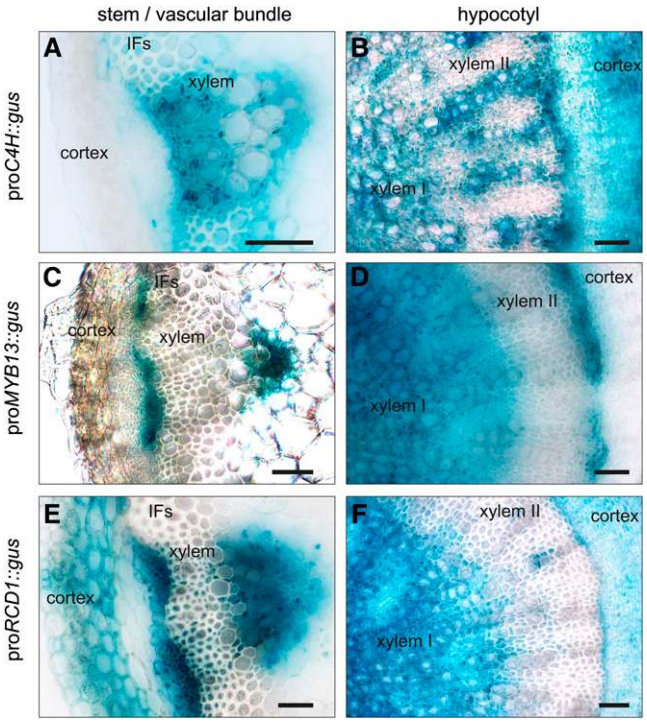

Figure 8. Localization of *C4H*, *RCD1*, and *MYB13* Expression with a Histochemical GUS Reporter Assay in Xylem Parenchyma Cells of *Arabidopsis* Vascular Tissues.

(A) and **(B)** GUS activity in transverse sections of pro*C4H*:*GUS* plant stem **(A)** and hypocotyl **(B)**.
(C) and **(D)** GUS activity in transverse sections of pro*MYB13*:*GUS* plant stem **(C)** and hypocotyl **(D)**.
(E) and **(F)** GUS activity in transverse sections of pro*RCD1*:*GUS* plant stem **(E)** and hypocotyl **(F)**.
IFs, interfascicular fibers. Bars = 50 μm.

DISCUSSION

The results presented here define several aspects of lignification and cell death of TEs. First of all, cell death of maturing TEs was shown to occur independently of their lignification status in *Z. elegans* xylogenic cell cultures (Figure 1). Lignification is therefore neither an inducer nor a prerequisite for TE PCD. Second, preventing cell death of maturing TEs was shown to inhibit TE cell wall lignification (Figure 3). Third, TEs were shown to retain the capacity to deposit lignin long after TE lifespan both in vitro (Figure 1) and in planta (Figure 2). Postmortem TE lignification was hypothesized quite some time ago in both whole plants (Stewart, 1966) and xylogenic cell cultures (Hosokawa et al., 2001; Tokunaga et al., 2005). Our results provide both experimental evidence and in situ demonstrations in in vitro TEs and in planta to support this hypothesis.

Postmortem TE lignification is counterintuitive since living cells are required for biosynthesis and the export of lignin monomers as well as for the production of other substrates (hydrogen peroxide and O_2^-) to the highly stable monolignol oxidizing enzymes (laccases and/or peroxidases) bound to the TE cell wall. Our results in both TE cell cultures and in planta suggest that the parenchymatic non-TE cells that surround the dead TEs participate in the TE lignification process. They were shown to not only express the lignin monomer biosynthetic genes (Figures 5, 6, and 8; see Supplemental Figures 4 and 5 online), but also to have the capacity to produce and export monolignols into the apoplast (Figure 7). They also express genes that, when mutated in *Arabidopsis*, affect the overall lignin chemistry of xylem tissues (Figure 9). We therefore propose that the parenchymatic cells of the xylem express specific genes to act as nurse cells to enable postmortem TE lignification. Similar ideas about cell cooperation during lignification were proposed on the basis of some earlier studies in *Z. elegans* TE cell cultures where an overall increase in lignin content of the cultures was reported in conditions when all the TEs were seemingly dead and the only living cells were the non-TEs (Hosokawa et al.,

2001; Tokunaga et al., 2005). Another example supporting cell cooperation during lignification comes from *Populus* trees, where it was recently shown that lignin composition of xylem fibers depended on its immediate surroundings in the wood, exhibiting an enrichment in G-type in its wall next to TEs and an enrichment in S-type lignin in its wall next to another fiber (Gorzsás et al., 2011). Therefore, it seems possible that cell-to-cell interaction is a fundamental aspect of lignification in all xylem elements.

The mechanisms by which monolignols are transported and incorporated into TE secondary walls are not known. It has been suggested that incorporation of monolignols is guided by cell wall localization of oxidizing enzymes but questioned by the fact that these enzymes have been identified in the secondary walls only after initiation of lignification (Donaldson, 2001). Our work supports that the sites of lignin deposition are indeed determined before lignification is initiated as addition of monolignols to dead PA-treated cells induced lignification of only the TE secondary cell walls (Figure 1). Targeting could be due to the presence of monolignol oxidizing enzymes, but it is possible that other factors, such as the presumed lignin nucleation sites (Boerjan et al., 2003), are important in this process as well. These monolignol oxidizing enzymes (laccases and/or peroxidases) could be produced in TEs prior to PCD and/or provided by the non-TE cells. An alternative scenario is that both monolignols and the oxidizing enzymes are more or less evenly distributed in the TE wall and that polymerization is triggered by a signal coming from the non-TEs in response to TE cell death. This signal could be for instance ROS that are known to be required for TE lignification (Karlsson et al., 2005) and to accumulate extensively in non-TEs of *Z. elegans* cell cultures and in xylem parenchyma of whole plants (Ros Barceló, 2005; Gómez Ros et al., 2006). Our result further clarified the role of ROS during TE postmortem lignification as they were shown to be produced by the non-TE cells via NADPH oxidase (Figure 7). Even though the details of monolignol transport and the exact identity of the signals inducing lignin polymerization remain unsolved, it is evident that TE lignification relies on interactions with other cells of the xylem, at least after TE cell death, and that ROS signaling is an important part of this.

Considering that TEs lignify after their cell death, it can be assumed that a large number of genes must be involved in the regulation of TE lignification in a non-cell-autonomous manner. We combined a differential screening method in the *Z. elegans* TE cell culture system with a functional assay in *Arabidopsis* and identified 10 non-TE expressed genes that had an effect on lignin content and/or composition (see Supplemental Data Set 2 online). One of the genes was *RCD1*, which has earlier been implicated in ozone-induced PCD by controlling ROS release and the concomitant hypersensitive response-like PCD response (Overmyer et al., 2000). A mutation in *RCD1* affected both total accumulation of lignin and composition, and it seems

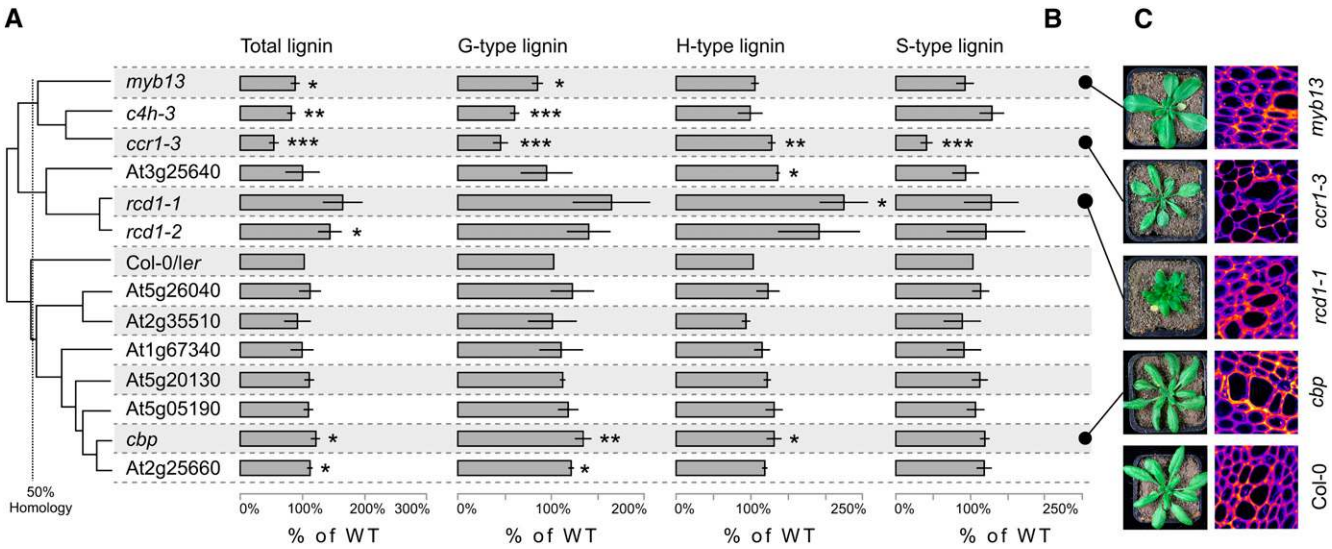

Figure 9. Reverse Genetic Analysis of a Selected Set of *Arabidopsis* Non-TE Expressed Genes by Py-GC/MS Analysis.

(A) Relative proportion of total lignin, H-type lignin, G-type lignin, and S-type lignin in the secondary walls of 2-month-old hypocotyls. The results are shown for the *Arabidopsis* mutants as a percentage of the wild-type (WT) control. Two lignin monomer biosynthetic mutants, *ccr1-3* and *c4h-3*, were included as a control. All mutants were in Columbia-0 background except for *myb13*, which was in Landsberg *erecta* background. Hierarchical clustering analysis of the average Py-GC/MS profiles of the mutants is shown on the left-hand side of the graph. For detailed description of the mutants, see Supplemental Data Set 2 online. The asterisks indicate statistically significant difference from the wild type by *t* test with Welch correction (*$P < 0.05$, **$P < 0.01$, and ***$P < 0.001$). Error bars indicate ±SD.

(B) Images of 4-week-old plants show that rosette size of the *rcd1-1* mutant was smaller than in the wild type, while *myb13* and *cbp* mutants grew normally compared with the corresponding wild type.

(C) UV confocal microscopy of transverse sections of the hypocotyl revealed no changes in the anatomy of any of the *rcd1-1*, *cbp*, and *myb13* mutants compared with the corresponding wild type. Autofluorescence of the secondary xylem is visualized by artificial color intensity scale.

possible that RCD1 is required to define the appropriate level of ROS production during lignin polymerization. Another interesting gene that appeared from the screen was *MYB13*, which belongs to R2R3 MYB gene family subgroup 2 together with *MYB14* and *MYB15*. MYB13 is closely related to subgroup 3 MYB58 and MYB63, which have been implicated in transcriptional regulation of lignin monomer biosynthetic genes (Zhou et al., 2009; Dubos et al., 2010). Very little is known about the function of the S2 subgroup MYBs except for that MYB15 has been shown to be involved in freezing tolerance (Agarwal et al., 2006). An S2 subgroup homolog in tobacco (*Nicotiana tabacum*), Nt-MYB2, was shown to activate transcription of phenylpropanoid biosynthetic Phe ammonia lyase (Sugimoto et al., 2000). These data, together with the observed alteration in lignin chemistry of the *MYB13* mutant, suggest that the S2 members of the MYB family are positive regulators of the phenylpropanoid pathway. Further studies are nevertheless required to show whether their function is directly related to postmortem TE lignification or to a more general function in lignification of xylem elements.

METHODS

Plant Material, Growth Conditions, and Xylogenic Cell Cultures

Zinnia elegans plants were grown at 25°C and 70% humidity in a 16/8-h light regime illuminated at 200 μmol m^{-2} s^{-1}. The first pair of leaves from 14-d-old seedlings of *Z. elegans* cv Envy (Hem Zaden) were used to isolate mesophyll cells for xylogenic cell suspension cultures according to the method of Fukuda and Komamine (1980). Cells were cultured in induction medium (C_{A+C}) containing 0.1 mg/L α-naphthylacetic acid and 0.2 mg/L benzyladenine (Sigma-Aldrich).

The SALK, SM, GABI, SAIL, and ET203 *Arabidopsis thaliana* mutant lines were obtained from the SALK Institute Genomic Analysis Laboratory. *sro1-1* (SALK_074525), *rcd1-1* (Ahlfors et al., 2004), and *rcd1-2* (Fujibe et al., 2004) were obtained from the laboratory of Jaakko Kangasjärvi. The *c4 h-3* (*ref3.3*; Ruegger and Chapple, 2001) and *ccr1-3* (SALK_123689; Mir Derikvand et al., 2008) mutants were a kind gift from Wout Boerjan. At1g06180 and its wild-type control were in the Landsberg *erecta* ecotype, while all the others were in Columbia-0 ecotype. Plants were grown 6 weeks under short-day conditions (8/16-h day/night photoperiod, 22°C/19°C temperature, and 75% relative humidity) in order to promote thickening of the hypocotyls. They were then transferred to long-day conditions (16/8-h day/night photoperiod, 22°C/19°C temperature, and 75% relative humidity) for four additional weeks. After the end of the growth period, the hypocotyls of the flowering plants were harvested and freeze-dried for the Py-GC/MS analysis or fixed in FAA (50% ethanol, 10% formaldehyde, and 5% acetic acid) for anatomical observation by confocal UV imaging. The plant material was divided into three growth batches, as defined in Supplemental Data Set 2 online.

Transgenic promoter:GUS reporter lines were created for *C4H* and *MYB13* in the *Arabidopsis* Columbia-0 background by floral dipping with transformed *Agrobacterium tumefaciens* LBA4404 (Clough and Bent, 1998). At least 2-kb genomic fragments of the promoters were cloned using BP cloning into Gateway-compatible entry vector pDONR207, with Phusion Taq polymerase (Finnzymes), and verified by sequencing. The primers were, for MYB13, forward 5′-GGGGACAAGTTTGTACAAAAAAGCAGGCTTGCAGGCCGGTGGTTAGTTACAG-3′/reverse 5′-GGGGACCACTTTGTACAAGAAAGCTGGGTAAAGTAACTAGTAAGTGTACGATGGC-3′ and, for C4H, forward 5′-GGGGACAAGTTTGTACAAAAAAGCAGGCTTGCTGTTGACAATACACTTATG-3′/reverse 5′-GGGGACCACTTTGTACAAGAAAGCTGGGTAGGAAGAAATAAAGAAGGGAG-3′. The promoter fragments were cloned by LR cloning into the binary destination vector pKGWFS7. The pro*RCD1*:*GUS* lines are described by Jaspers et al. (2009).

Z. elegans epicotyls were collected for Maüle staining and in situ multiplex RT-PCR analysis from 3-week-old seedlings grown in long-day conditions.

The middle part of *Z. elegans* epicotyl internodes was collected for FT-IR analysis from 5-week-old plants and directly frozen in liquid nitrogen. Cryosections were taken at 16 and 20 μm with a cryomicrotome (Microm HM 505 E).

Mature xylem tissues were collected for thioacidolysis from *Pinus sylvestris* and *Populus tremula x alba* by scraping from the surface of the wood after peeling of the bark and removal of the early differentiating xylem tissues.

Pharmacological Treatments

Pharmacological treatments of cell cultures were performed with STS and Cat in water or PA, NAC, and DPI in DMSO. Treatments were performed either on 12-mL cultures in 50-mL erlenmeyer flasks or on 1-mL cultures in 12-well plates and included initial treatment with pharmacological compound(s). Lignification postmortem was performed by supplying 144-h-old PA-treated TEs with 60 μM coniferyl alcohol and/or 60 μM sinapyl alcohol solubilized in DMSO and/or 1 mM NAC, 15 μM DPI, or 1 mg/mL Cat or with 0.2 μm filtered extracellular medium from 120-h-old cells for 48 h, followed by lignin staining by phloroglucinol-HCl or FT-IR analysis.

Cytological and Histological Imaging and Quantification

Simultaneous staining for cell viability, cellulose, and lignin in secondary cell walls of developing TEs was performed as described previously (Pesquet and Tuominen, 2011). Quantification was performed for five replicate samples with 200 to 300 cells in each sample. Lignification of cryosections or TE cell cultures was estimated by staining with phloroglucinol-HCl staining (1% phloroglucinol in 47.5% ethanol and 1.5 M HCl) (Crocker, 1921; Pomar et al., 2002). For staining of the cell cultures, 100 μL cell suspension was pelleted by centrifugation at 200*g* for 2 min and stained at room temperature for 5 min before mounting between slide and cover slip and immediate imaging. For quantification purposes, only intensely stained cells were counted (Tokunaga et al., 2005). Maüle staining was performed according to Crocker (1921) on hand sections taken from *Z. elegans* epicotyls.

Confocal UV lignin imaging/distribution was performed with a confocal Leica SP2 on a Leica DM IRE2 inverted microscope with excitation laser diode 405 nm in a 450- to 510-nm emission window. Lignin distribution analysis and artificial color scaling of the gray-scale values were performed using ImageJ (http://rsbweb.nih.gov/ij/). Lignin distribution was measured by 10 independent measurements for each cell wall position in five independent images and was expressed as a percentage of the total lignin fluorescence. Lignin autofluorescence emission spectra were obtained with excitation at 405 nm and a 10-nm-wide emission window between 410 and 710 nm. Lignin autofluorescence spectra were expressed as a percentage of their maximum gray-scale emission value and measured by 10 independent measurements for each cell wall position in five independent images using the ImageJ software. Spectra between vessel secondary cell wall, fiber secondary cell wall, compound middle lamella, and cell corner did not show any differences.

Histochemical GUS staining of the *Arabidopsis* pro*RCD1*:*GUS*, pro*MYB13*:*GUS*, and pro*C4H*:*GUS* was performed on fresh hand sections taken from 2-month-old stem and hypocotyl material according to Muñiz et al. (2008).

TUNEL Labeling

Terminal deoxynucleotidyl transferase–mediated dUTP–fluorescein isothiocyanate (FITC) nick end labeling was assessed in TEs of comparable developmental stages 60 and 72 h after TE induction for the control and

STS-treated TEs, respectively. The TEs were embedded in 2% low-melting agarose beads fixed in freshly prepared 4% paraformaldehyde in PBS, pH 7.4, and processed with the TUNEL staining kit according to the manufacturer's instructions (Roche Applied Science). Samples were observed with a confocal Leica SP2 on a Leica DM IRE2 inverted microscope for FITC/TUNEL staining with the 488-nm argon excitation laser in an emission window of 500 to 550 nm and for the 0.1% calcofluor-stained cell walls with a 405-nm diode excitation laser in an emission window of 410 to 450 nm. Image analysis was performed with ImageJ.

FT-IR Microspectroscopy

FT-IR spectra of *Z. elegans* cell cultures were recorded with a Bruker Equinox 55 spectrometer equipped with a Hyperion 3000 microscopy accessory (Bruker Optics) using a liquid nitrogen–cooled single-element (SE) HgCdTe detector and a Sony Exwave HAD color digital video camera for positioning. Prior to FT-IR measurements, TEs were transferred to infrared transparent polished rectangular BaF_2 windows (30 × 15 × 4 mm; International Crystal Laboratories) and dried in a desiccator for 48 h. For measurements, individual TEs were selected by rectangular knife-edge apertures masking off the remaining parts of the image area. FT-IR spectra of *Z. elegans* stem cryosections were recorded with a Bruker Tensor 27 spectrometer equipped with a Hyperion 3000 microscopy accessory (Bruker Optics) using a liquid nitrogen–cooled focal plane array (FPA) detector and a Sony Exwave HAD color digital video camera for positioning. Prior to FT-IR measurements, cryosections were washed in distilled water, transferred to infrared transparent polished rectangular CaF_2 slides (75 × 25 × 1 mm; Crystran), and dried in a desiccator for 1 week. The sample tray was boxed, and the chamber was continuously purged with dry air. Spectra were recorded in a transmission mode over the range of 400 to 4000 cm^{-1} (SE) or 900 to 4000 cm^{-1} (FPA) with a spectral resolution of 4 cm^{-1}. For each spectrum, 1024 (SE) or 32 (FPA) interferograms were coadded to obtain high signal-to-noise ratios. Prior to sample measurements, background spectra were recorded for each sample at a nearby empty spot on the BaF_2 crystal using 512 (SE) or 32 (FPA) scans. For SE, spectral treatment included conversion to data point table files using OPUS (version 5.0.53; Bruker Optik) and a two-point linear baseline correction between 700 and 1900 cm^{-1} and a total sum (area) normalization over the same spectral range using custom scripts programmed within the MATLAB software (version 7.0; Mathworks). For FPA, spectral treatment included automatic 64-point rubber band baseline correction (excluding CO_2 bands) and vector normalization over the 900- and 1800-cm^{-1} spectral range using OPUS (version 7.0). Multivariate analysis of baseline-corrected and normalized spectra was performed using SIMCA-P+ (12.0; Umetrics) as previously described by Gorzsás et al. (2011). For each sample, eight to 12 individual cells were recorded by SE. From each FPA image, six to 16 spectra were extracted, with one spectrum/vessel element/image. Hierarchical clustering of the average FT-IR spectra was performed using HCE 3.5 software (hierarchical clustering explorer 3.5; http://www.cs.umd.edu/hcil/hce/). From the spectra, 1510-cm^{-1} average peak area was calculated for each monitored xylem vessel. Statistically significant differences ($P < 0.05$) between xylem vessels and differences between internodes were sought by two-way analysis of variance (ANOVA). A post-ANOVA Tukey test was used to detect significant differences ($P < 0.05$) pairwise between vessel types within and between internodes.

RNA Extraction

Cell suspensions were pelleted by centrifugation for 5 min at 150*g*. Culture medium was removed, and cell pellets were frozen in liquid nitrogen. Grinding of cell samples was performed by adding two to three tungsten carbide beads (Qiagen) and vortexing cells for 20 s between three consecutive freeze-thaw events. One milliliter of TRIreagent (MRC) was added to the ground cells. Total RNA was isolated according to the manufacturer's instructions and subjected to DNA digestion with 5 units of RNase-free DNase I (Promega) for 1 h at 37°C. A second round of RNA extraction was performed as indicated above. RNA was quantified using an RNA Biophotometer (Eppendorf) and visualized after electrophoresis on 1.5% agarose gels.

Construction of Subtractive Libraries by SSH

SSH libraries were constructed using a SMART-PCR cDNA synthesis kit (Clontech) for cDNA synthesis and a PCR-Select cDNA subtraction kit (Clontech) for the subtraction step. First-strand cDNAs were prepared from 1 μg of total RNA from *Z. elegans* cell suspensions cultured for 60 and 72 h (without STS) or 60 and 72 h (with 60 μM STS). Double-stranded cDNA were obtained by PCR according to the manufacturer's instructions. Amplification, subtraction, and preliminary screening were performed as previously described by Diatchenko et al. (1996) and Pesquet et al. (2005).

Sequencing of the SSH Libraries

The obtained libraries were sequenced as described by Laitinen et al. (2005). Briefly, colonies were picked and grown in 96-deep-well plates overnight. Plasmids were purified with isopropanol precipitation, and inserts were amplified using vector universal primers. The amplified products were purified and sequenced using BigDye Terminator Chemistry v3.1 and analyzed on an ABI 3730 sequencer (Applied Biosystems).

SSH Library Database Construction

All sequence chromatograms were transformed using Chromas software (http://www.technelysium.com.au/) batch export in a fasta format file. A total of 2625 single pass sequences were generated. Vector and adapter sequences were removed using Chromas software, and the cleaned sequences were clustered to eliminate redundancy resulting in 651 nonredundant ESTs. Homology analyses were performed on nonredundant EST sequences to (1) identify known *Z. elegans* sequences by BLASTn (e score < 1e-3), (2) determine closest *Arabidopsis* homolog by BLASTx (e score < 1e-3) and BLASTn (e score < 1e-3) on The Arabidopsis Information Resource protein BLAST data sets, (3) determine closest plant homolog by BLASTx (e score < 1e-3) on The Arabidopsis Information Resource protein BLAST data sets, and (4) determine closest protein homolog by BLASTx (e score < 1e-3) on GenBank protein BLAST data set nr.

Quantitative, Classical, and Multiplex in Situ RT-PCR

Total RNA from cells harvested at different time points along the culture period were isolated as described above. cDNA was prepared using oligo (dT) and random primers and 1 μg of RNA as template. All primers were synthesized by Invitrogen. Classical RT-PCR was performed using 1:5 diluted cDNA with Invitrogen Taq polymerase for 25 to 40 cycles depending on the gene analyzed. Quantitative RT-PCR was conducted using 1:40 diluted cDNA, iQ SYBR Green Supermix, and 5 pmol of each primer. Primer sequences are listed in Supplemental Data Set 3 online. PCR cycles for Bio-Rad iQ5 multicolor real-time PCR detection system were as follows: initial denaturation at 95°C for 3 min, denaturation at 95°C for 10 s, and annealing at 55°C for 30 s for 40 cycles. *Z. elegans 18S* rRNA gene was used as a reference. The same cDNA was used for each individual quantitative RT-PCR plate with three technical repeats for each gene. The average cycle threshold (C_t) value of the *18S* gene was subtracted from the corresponding C_t value of each gene to obtain a ΔC_t value, and the relative expression levels were calculated with the equation $2^{-\Delta Ct}$.

Multiplex in situ RT-PCR was performed according to Pesquet et al. (2004) with forward primer 5′-labeled with FITC, tetramethylrhodamine anhydride (TMRA), or Cy5 and unlabeled reverse primer. The primer sequences are listed in Supplemental Data Set 3 online. Samples were observed with a confocal Leica SP2 on a Leica DM IRE2 inverted microscope with a 488-nm excitation laser argon in an emission window of 500 to 550 nm for FITC detection, with a 561-nm excitation laser diode in an emission window of 580 to 630 nm for TMRA detection, and with a 633-nm excitation laser HeNe in an emission window of 660 to 710 nm for Cy5 detection. Image analysis and processing were performed using ImageJ.

Py-GC/MS Analysis

Freeze-dried hypocotyls were ball-milled (MM400; Retsch) at 30 Hz in stainless steel jars (1.5 mL) for 2 min with one ball (diameter of 7 mm). A total of 35 to 50 μg of powder was then applied to the online pyrolizer (PY-2020iD and AS1020E; FrontierLabs) mounted on a gas chromatograph/mass spectrometer (7890A/5975C; Agilent Technologies). Pyrolysis was conducted at 450°C. The pyrolysate was separated on a capillary column with a length of 30 m, diameter of 250 μm, and film thickness of 25 μm (JandW DB-5; Agilent Technologies Sweden). The gas chromatography oven temperature program started at 40°C, followed by an temperature ramp of 32°C/min to 100°C, 6°C/min to 118.75°C, 15°C/min to 250°C, and 32°C/min to 320°C. Total run time was 19 min and full-scan spectra were recorded in the range of 35 to 250 mass-to-charge ratio. Data processing, including peak detection, integration, normalization, and identification, was done as described by Gerber et al. (2012).

The relative amounts of S-, G-, and H-lignin, the carbohydrates, and the S/G lignin ratio were further expressed as a percentage of the amounts in corresponding wild-type plants of the same growth batch that was analyzed at the same time. SIMCA-P+ (12.0; Umetrics) was used for multivariate sample classification based on Py-GC/MS fingerprints by orthogonal partial least square discriminant analysis (Bylesjö et al., 2006). In all the models, the number of components was set to one principal component plus two orthogonal components. Hierarchical clustering of mutants with strong predictive orthogonal partial least square discriminant analysis models ($Q2 > 0.5$) was performed on the average amounts of the pyrolysis fragments for each mutant using HCE 3.5 software (http://www.cs.umd.edu/hcil/hce/), while principal component analysis of each individual replicate was performed using SIMCA-P+ (12.0).

In Silico Analysis

Publicly available normalized Affymetrix microarray gene expression data from Kubo et al. (2005) were obtained from ArrayExpress and transferred to Microsoft Excel to monitor candidate gene expression profiles throughout TE differentiation. Gene expression profiles of all 50 candidate genes and secondary cell wall and PCD markers were displayed by hierarchical clustering with HCE 3.5 software (http://www.cs.umd.edu/hcil/hce/).

Accession Numbers

All SSH sequences were deposited in the EMBL EST database (accession numbers FM879143 to FM881767). Other genes studied in this article include *C4H* (At2g30490), *CCR1* (AT1G15950), *RCD1* (At1g32230), and *MYB13* (At1g06180).

Supplemental Data

The following materials are available in the online version of this article.

Supplemental Figure 1. TE Lignification in *Zinnia* TE Cultures and in Planta.

Supplemental Figure 2. Multivariate Analysis of FT-IR Spectra from the Primary Xylem Vessels of Whole *Zinnia* Plants.

Supplemental Figure 3. Cell Cytology in Response to STS Treatment in *Zinnia* TE Cultures.

Supplemental Figure 4. Multiplex in Situ RT-PCR of CINNAMOYL COA REDUCTASE and CINNAMYL ALCOHOL DEHYDROGENASE in Cross Sections of *Zinnia elegans* Epicotyl.

Supplemental Figure 5. In Silico Analysis of SSH Clones during *Zinnia* and *Arabidopsis* TE Differentiation.

Supplemental Figure 6. Confocal UV Spectroscopy Analysis of the Secondary Xylem in Hypocotyls of Selected 2-Month-Old *Arabidopsis* Mutants.

Supplemental Data Set 1. Bioinformatic Analysis of *Zinnia elegans* ESTs.

Supplemental Data Set 2. Pyrolysis–Gas Chromatography/Mass Spectrometry Analysis of Hypocotyls in 2-Month-Old Wild-Type and Mutant Plants.

Supplemental Data Set 3. Primers Used for Classical RT-PCR, Quantitative RT-PCR, and Multiplex in Situ RT-PCR.

ACKNOWLEDGMENTS

We thank Shinya Kajita for the thin layer chromatography analysis of thioacidolysis products of *Zinnia*, *Populus*, and *Pinus*. We also thank the Swedish Research Council Formas (Research Program on Wood Material Science, the FuncFiber Center of Excellence in Wood Science, and the Strong Research Environment BioImprove), the Swedish research council Vetenskapsrådet and the Swedish Governmental Agency for Innovation Systems Vinnova (Umeå Plant Science Centre Berzelii Centre), Bio4Energy (a strategic research environment appointed by the Swedish government), the Carl Trygger Foundation, the Kempe Foundation, and the Finnish Funding Agency for Technology and Innovation Tekes for financial support. We are also grateful to the Plant Cell Wall and Carbohydrate Analytical Facility at the Umeå Plant Science Centre/Sveriges lantbruksuniversitet, supported by Bio4Energy and TC4F projects.

AUTHOR CONTRIBUTIONS

E.P., B.Z., D.G., and H.T. conceived and designed the experiments. E.P., B.Z., T.P., O.B., H.S., S.E., A.G., C.C.-M., and E.A. performed the experiments. E.P., B.Z., L.G., S.E., E.A., and H.T. analyzed the data. E.P., L.P., J.K., B.S., D.G., and H.T. contributed reagents/materials/analysis tools. E.P. and H.T. wrote the article.

Received February 8, 2013; revised March 12, 2013; accepted March 21, 2013; published April 9, 2013.

REFERENCES

Agarwal, M., Hao, Y., Kapoor, A., Dong, C.-H., Fujii, H., Zheng, X., and Zhu, J.-K. (2006). A R2R3 type MYB transcription factor is involved in the cold regulation of CBF genes and in acquired freezing tolerance. J. Biol. Chem. **281:** 37636–37645.

Ahlfors, R., Lång, S., Overmyer, K., Jaspers, P., Brosché, M., Tauriainen, A., Kollist, H., Tuominen, H., Belles-Boix, E., Piippo, M., Inzé, D., Palva, E.T., and Kangasjärvi, J. (2004). Arabidopsis RADICAL-INDUCED CELL DEATH1 belongs to the WWE protein-protein interaction domain protein family and modulates abscisic acid, ethylene, and methyl jasmonate responses. Plant Cell **16:** 1925–1937.

Alejandro, S., Lee, Y., Tohge, T., Sudre, D., Osorio, S., Park, J., Bovet, L., Lee, Y., Geldner, N., Fernie, A.R., and Martinoia, E. (2012). AtABCG29 is a monolignol transporter involved in lignin biosynthesis. Curr. Biol. **22:** 1207–1212.

Baghdady, A., Blervacq, A.S., Jouanin, L., Grima-Pettenati, J., Sivadon, P., and Hawkins, S. (2006). *Eucalyptus gunnii* CCR and CAD2 promoters are active in lignifying cells during primary and secondary xylem formation in *Arabidopsis thaliana*. Plant Physiol. Biochem. **44:** 674–683.

Boerjan, W., Ralph, J., and Baucher, M. (2003). Lignin biosynthesis. Annu. Rev. Plant Biol. **54:** 519–546.

Bylesjö, M., Rantalainen, M., Cloarec, O., Nicholson, J.K., Holmes, E., and Trygg, J. (2006). OPLS discriminant analysis: Combining the strengths of PLS-DA and SIMCA classification. J. Chemometr. **20:** 341–351.

Chen, C.Y., Meyermans, H., Burggraeve, B., De Rycke, R.M., Inoue, K., De Vleesschauwer, V., Steenackers, M., Van Montagu, M.C., Engler, G.J., and Boerjan, W.A. (2000). Cell-specific and conditional expression of caffeoyl-coenzyme A-3-O-methyltransferase in poplar. Plant Physiol. **123:** 853–867.

Clough, S.J., and Bent, A.F. (1998). Floral dip: a simplified method for Agrobacterium-mediated transformation of *Arabidopsis thaliana*. Plant J. **16:** 735–743.

Crocker, E.C. (1921). An experimental study of the significance of "lignin" color reactions. Ind. Eng. Chem. **13:** 625–627.

Demura, T., et al. (2002). Visualization by comprehensive microarray analysis of gene expression programs during transdifferentiation of mesophyll cells into xylem cells. Proc. Natl. Acad. Sci. USA **99:** 15794–15799.

Diatchenko, L., Lau, Y.F.C., Campbell, A.P., Chenchik, A., Moqadam, F., Huang, B., Lukyanov, S., Lukyanov, K., Gurskaya, N., Sverdlov, E.D., and Siebert, P.D. (1996). Suppression subtractive hybridization: a method for generating differentially regulated or tissue-specific cDNA probes and libraries. Proc. Natl. Acad. Sci. USA **93:** 6025–6030.

Donaldson, L.A. (2001). Lignification and lignin topochemistry - An ultrastructural view. Phytochemistry **57:** 859–873.

Dubos, C., Stracke, R., Grotewold, E., Weisshaar, B., Martin, C., and Lepiniec, L. (2010). MYB transcription factors in *Arabidopsis*. Trends Plant Sci. **15:** 573–581.

Faix, O. (1991). Classification of lignins from different botanical origins by FT-IR spectroscopy. Holzforschung **45:** 21–27.

Fujibe, T., Saji, H., Arakawa, K., Yabe, N., Takeuchi, Y., and Yamamoto, K.T. (2004). A methyl viologen-resistant mutant of Arabidopsis, which is allelic to ozone-sensitive *rcd1*, is tolerant to supplemental ultraviolet-B irradiation. Plant Physiol. **134:** 275–285.

Fukuda, H. (1997). Programmed cell death during vascular system formation. Cell Death Differ. **4:** 684–688.

Fukuda, H., and Komamine, A. (1980). Direct evidence for cytodifferentiation to tracheary elements without intervening mitosis in a culture of single cells isolated from the mesophyll of *Zinnia elegans*. Plant Physiol. **65:** 61–64.

Gerber, L., Eliasson, M., Trygg, J., Moritz, T., and Sundberg, B. (2012). Multivariate curve resolution provides a high-throughput data processing pipeline for pyrolysis-gas chromatography/mass spectrometry. J. Anal. Appl. Pyrolysis **95:** 95–100.

Gómez Ros, L.V., Paradiso, A., Gabaldón, C., Pedreño, M.A., de Gara, L., and Ros Barceló, A. (2006). Two distinct cell sources of H_2O_2 in the lignifying *Zinnia elegans* cell culture system. Protoplasma **227:** 175–183.

Gorzsás, A., Stenlund, H., Persson, P., Trygg, J., and Sundberg, B. (2011). Cell-specific chemotyping and multivariate imaging by combined FT-IR microspectroscopy and orthogonal projections to latent structures (OPLS) analysis reveals the chemical landscape of secondary xylem. Plant J. **66:** 903–914.

Hosokawa, M., Suzuki, S., Umezawa, T., and Sato, Y. (2001). Progress of lignification mediated by intercellular transportation of monolignols during tracheary element differentiation of isolated Zinnia mesophyll cells. Plant Cell Physiol. **42:** 959–968.

Hu, W.J., Kawaoka, A., Tsai, C.J., Lung, J.H., Osakabe, K., Ebinuma, H., and Chiang, V.L. (1998). Compartmentalized expression of two structurally and functionally distinct 4-coumarate:CoA ligase genes in aspen (*Populus tremuloides*). Proc. Natl. Acad. Sci. USA **95:** 5407–5412.

Jaspers, P., Blomster, T., Brosché, M., Salojärvi, J., Ahlfors, R., Vainonen, J.P., Reddy, R.A., Immink, R., Angenent, G., Turck, F., Overmyer, K., and Kangasjärvi, J. (2009). Unequally redundant RCD1 and SRO1 mediate stress and developmental responses and interact with transcription factors. Plant J. **60:** 268–279.

Jones, L., Ennos, A.R., and Turner, S.R. (2001). Cloning and characterization of irregular xylem4 (irx4): a severely lignin-deficient mutant of *Arabidopsis*. Plant J. **26:** 205–216.

Karlsson, M., Melzer, M., Prokhorenko, I., Johansson, T., and Wingsle, G. (2005). Hydrogen peroxide and expression of hipI-superoxide dismutase are associated with the development of secondary cell walls in *Zinnia elegans*. J. Exp. Bot. **56:** 2085–2093.

Kenrick, P., and Crane, P.R. (1997). The origin and early evolution of plants on land. Nature **389:** 33–39.

Kubo, M., Udagawa, M., Nishikubo, N., Horiguchi, G., Yamaguchi, M., Ito, J., Mimura, T., Fukuda, H., and Demura, T. (2005). Transcription switches for protoxylem and metaxylem vessel formation. Genes Dev. **19:** 1855–1860.

Lacombe, E., Van Doorsselaere, J., Boerjan, W., Boudet, A.M., and Grima-Pettenati, J. (2000). Characterization of cis-elements required for vascular expression of the cinnamoyl CoA reductase gene and for protein-DNA complex formation. Plant J. **23:** 663–676.

Laitinen, R.A.E., Immanen, J., Auvinen, P., Rudd, S., Alatalo, E., Paulin, L., Ainasoja, M., Kotilainen, M., Koskela, S., Teeri, T.H., and Elomaa, P. (2005). Analysis of the floral transcriptome uncovers new regulators of organ determination and gene families related to flower organ differentiation in *Gerbera hybrida* (Asteraceae). Genome Res. **15:** 475–486.

Lauvergeat, V., Rech, P., Jauneau, A., Guez, C., Coutos-Thevenot, P., and Grima-Pettenati, J. (2002). The vascular expression pattern directed by the *Eucalyptus gunnii* cinnamyl alcohol dehydrogenase EgCAD2 promoter is conserved among woody and herbaceous plant species. Plant Mol. Biol. **50:** 497–509.

Liu, C.J. (2012). Deciphering the enigma of lignification: Precursor transport, oxidation, and the topochemistry of lignin assembly. Mol. Plant **5:** 304–317.

Miao, Y.C., and Liu, C.J. (2010). ATP-binding cassette-like transporters are involved in the transport of lignin precursors across plasma and vacuolar membranes. Proc. Natl. Acad. Sci. USA **107:** 22728–22733.

Mir Derikvand, M., Sierra, J.B., Ruel, K., Pollet, B., Do, C.T., Thévenin, J., Buffard, D., Jouanin, L., and Lapierre, C. (2008). Redirection of the phenylpropanoid pathway to feruloyl malate in *Arabidopsis* mutants deficient for cinnamoyl-CoA reductase 1. Planta **227:** 943–956.

Muñiz, L., Minguet, E.G., Singh, S.K., Pesquet, E., Vera-Sirera, F., Moreau-Courtois, C.L., Carbonell, J., Blázquez, M.A., and Tuominen, H. (2008). ACAULIS5 controls *Arabidopsis* xylem specification through the prevention of premature cell death. Development **135:** 2573–2582.

Overmyer, K., Tuominen, H., Kettunen, R., Betz, C., Langebartels, C., and Sandermann, H., Jr.,., and Kangasjärvi, J. (2000). Ozone-sensitive *Arabidopsis* rcd1 mutant reveals opposite roles for ethylene and jasmonate signaling pathways in regulating superoxide-dependent cell death. Plant Cell **12:** 1849–1862.

Pesquet, E., Barbier, O., Ranocha, P., Jauneau, A., and Goffner, D. (2004). Multiple gene detection by in situ RT-PCR in isolated plant cells and tissues. Plant J. **39:** 947–959.

Pesquet, E., Jauneau, A., Digonnet, C., Boudet, A.M., Pichon, M., and Goffner, D. (2003). Zinnia elegans: The missing link from in vitro tracheary elements to xylem. Physiol. Plant. **119:** 463–468.

Pesquet, E., Jauneau, A., and Goffner, D. (2006). Zinnia elegans is an excellent model for xylogenesis: from in vitro and in planta. In Floriculture, Ornamental and Plant Biotechnology: Advances and Topical Issues, J.A.T. da Silva, ed (London: Global Science Books), pp. 171–178.

Pesquet, E., Korolev, A.V., Calder, G., and Lloyd, C.W. (2010). The microtubule-associated protein AtMAP70-5 regulates secondary wall patterning in *Arabidopsis* wood cells. Curr. Biol. **20:** 744–749.

Pesquet, E., and Lloyd, C. (2011). Microtubules, MAPs and xylem formation. In The Plant Cytoskeleton, B. Liu, ed (New York: Springer), pp. 277–306.

Pesquet, E., Ranocha, P., Legay, S., Digonnet, C., Barbier, O., Pichon, M., and Goffner, D. (2005). Novel markers of xylogenesis in zinnia are differentially regulated by auxin and cytokinin. Plant Physiol. **139:** 1821–1839.

Pesquet, E., and Tuominen, H. (2011). Ethylene stimulates tracheary element differentiation in *Zinnia elegans* cell cultures. New Phytol. **190:** 138–149.

Pickett-Heaps, J.D. (1968). Xylem wall deposition. Protoplasma **65:** 181–205.

Pomar, F., Merino, F., and Barceló, A.R. (2002). O-4-Linked coniferyl and sinapyl aldehydes in lignifying cell walls are the main targets of the Wiesner (phloroglucinol-HCl) reaction. Protoplasma **220:** 17–28.

Ralph, J. (2010). Hydroxycinnamates in lignification. Phytochem. Rev. **9:** 65–83.

Ros Barceló, A. (2005). Xylem parenchyma cells deliver the H_2O_2 necessary for lignification in differentiating xylem vessels. Planta **220:** 747–756.

Ruegger, M., and Chapple, C. (2001). Mutations that reduce sinapoylmalate accumulation in *Arabidopsis thaliana* define loci with diverse roles in phenylpropanoid metabolism. Genetics **159:** 1741–1749.

Sato, Y., Sugiyama, M., Górecki, R.J., Fukuda, H., and Komamine, A. (1993). Interrelationship between lignin deposition and the activities of peroxidase isoenzymes in differentiating tracheary elements of Zinnia. Planta **189:** 584–589.

Schalk, M., Cabello-Hurtado, F., Pierrel, M.A., Atanossova, R., Saindrenan, P., and Werck-Reichhart, D. (1998). Piperonylic acid, a selective, mechanism-based inactivator of the trans-cinnamate 4-hydroxylase: A new tool to control the flux of metabolites in the phenylpropanoid pathway. Plant Physiol. **118:** 209–218.

Schoch, G.A., Nikov, G.N., Alworth, W.L., and Werck-Reichhart, D. (2002). Chemical inactivation of the cinnamate 4-hydroxylase allows for the accumulation of salicylic acid in elicited cells. Plant Physiol. **130:** 1022–1031.

Smart, C.C., and Amrhein, N. (1985). The influence of lignification on the development of vascular tissue in *Vigna radiata* L. Protoplasma **124:** 87–95.

Stewart, C.M. (1966). Excretion and heartwood formation in living trees. Science **153:** 1068–1074.

Sugimoto, K., Takeda, S., and Hirochika, H. (2000). MYB-related transcription factor NtMYB2 induced by wounding and elicitors is a regulator of the tobacco retrotransposon Tto1 and defense-related genes. Plant Cell **12:** 2511–2528.

Sundström, J.F., et al. (2009). Tudor staphylococcal nuclease is an evolutionarily conserved component of the programmed cell death degradome. Nat. Cell Biol. **11:** 1347–1354.

Thévenin, J., Pollet, B., Letarnec, B., Saulnier, L., Gissot, L., Maia-Grondard, A., Lapierre, C., and Jouanin, L. (2011). The simultaneous repression of CCR and CAD, two enzymes of the lignin biosynthetic pathway, results in sterility and dwarfism in *Arabidopsis thaliana*. Mol. Plant **4:** 70–82.

Tokunaga, N., Sakakibara, N., Umezawa, T., Ito, Y., Fukuda, H., and Sato, Y. (2005). Involvement of extracellular dilignols in lignification during tracheary element differentiation of isolated Zinnia mesophyll cells. Plant Cell Physiol. **46:** 224–232.

Wooding, F.B.P. (1968). Radioautographic and chemical studies of incorporation into sycamore vascular tissue walls. J. Cell Sci. **3:** 71–80.

Vanholme, R., Morreel, K., Darrah, C., Oyarce, P., Grabber, J.H., Ralph, J., and Boerjan, W. (2012). Metabolic engineering of novel lignin in biomass crops. New Phytol. **196:** 978–1000.

Zhou, J., Lee, C., Zhong, R., and Ye, Z.-H. (2009). MYB58 and MYB63 are transcriptional activators of the lignin biosynthetic pathway during secondary cell wall formation in *Arabidopsis*. Plant Cell **21:** 248–266.

Non-Cell-Autonomous Postmortem Lignification of Tracheary Elements in *Zinnia elegans*

Edouard Pesquet, Bo Zhang, András Gorzsás, Tuula Puhakainen, Henrik Serk, Sacha Escamez, Odile Barbier, Lorenz Gerber, Charleen Courtois-Moreau, Edward Alatalo, Lars Paulin, Jaakko Kangasjärvi, Björn Sundberg, Deborah Goffner and Hannele Tuominen

Plant Cell; originally published online April 9, 2013;
DOI 10.1105/tpc.113.110593